HHS Public Access

Author manuscript

Circulation. Author manuscript; available in PMC 2020 October 22.

Published in final edited form as:

Circulation. 2019 October 22; 140(17): 1409–1425. doi:10.1161/CIRCULATIONAHA.119.040629.

Phenotypically-Silent Bone Morphogenetic Protein Receptor 2 (*Bmpr2*) Mutations Predispose Rats to Inflammation-Induced Pulmonary Arterial Hypertension by Enhancing The Risk for Neointimal Transformation

Wen Tian, PhD[1,2,*], **Xinguo Jiang, MD PhD**[1,2,*], **Yon K. Sung, MD**[1,2], **Eric Shuffle, MS**[1,2], **Ting-Hsuan Wu, BS**[2], **Peter N. Kao, MD, PhD**[2], **Allen B. Tu, BS**[1,2], **Peter Dorfmüller, MD, PhD**[3,4,5], **Aiqin Cao, PhD**[2], **Lingli Wang, MD**[2], **Gongyong Peng, MD, PhD**[1,2,6], **Yesl Kim, MS**[1,2], **Patrick Zhang, BS**[1,2], **James Chappell, PhD**[2], **Shravani Pasupneti, MD**[1,2], **Petra Dahms, BS**[1,2], **Peter Maguire, BS**[2], **Hassan Chaib, PhD**[2], **Roham Zamanian, MD**[2], **Marc Peters-Golden, MD**[7], **Michael P. Snyder, PhD**[2], **Norbert F. Voelkel, MD**[8], **Marc Humbert, MD, PhD**[3,4,9], **Marlene Rabinovitch, MD**[2], **Mark R. Nicolls, MD**[1,2]

[1]VA Palo Alto Health Care System, Palo Alto, CA; [2]Stanford University School of Medicine, Stanford, CA; [3]Faculté de Médecine, Université Paris-Sud and Université Paris-Saclay, Le Kremlin-Bicêtre, France; [4]INSERM UMR_S 999, Le Plessis-Robinson, France; [5]Pathology Department, Hôpital Marie Lannelongue, Le Plessis-Robinson, Paris, France; [6]State Key Laboratory of Respiratory Diseases, Guangzhou Institute of Respiratory Health, The First Affiliated Hospital of Guangzhou Medical University, Guangzhou, China; [7]University of Michigan Health System, Ann Arbor, Michigan; [8]Free University Medical Center Amsterdam, the Netherlands; [9]AP-HP, Service de Pneumologie, Centre de Référence de l'Hypertension Pulmonaire Sévère, DHU Thorax Innovation, Hôpital de Bicêtre, Le Kremlin-Bicêtre, France

Abstract

Background: *Bmpr2* mutations are critical risk factors for hereditary pulmonary arterial hypertension (hPAH) with approximately 20% of carriers developing disease. There is an unmet medical need to understand how environmental factors, such as inflammation, render *Bmpr2* mutants susceptible to PAH. Overexpressing 5-lipoxygenase (5-LO) provokes lung inflammation and transient PAH in *Bmpr2*$^{+/-}$ mice. Accordingly, 5-LO and its metabolite, leukotriene B_4 (LTB_4), are candidates for the 'second hit'. The purpose of this study was to determine how 5-LO-

Addresses for Correspondence: Wen Tian, PhD, VA Palo Alto Health Care System, Stanford University School of Medicine, 3801 Miranda Ave, Bldg. 101, A4-151, Palo Alto, CA 94304, Tel: (650) 493-5000 x64771, amytian@stanford.edu, Mark R. Nicolls, MD, VA Palo Alto Health Care System, Stanford University School of Medicine, Med111P, 3801 Miranda Ave., Palo Alto, CA 94304, Tel: (650) 493-5000 x69289, Fax:(650)849-0553, mnicolls@stanford.edu.

Author contributions: WT and XJ planned and performed experiments and were responsible for data analysis. YS, ES, AT, PD, YK, SP, and GP performed experiments. TW, PM, and JC analyzed the RNAseq data. PD, AC, LW provided reagents. PK, HC, RZ, MPG, MPS, NFV, MR, and MH provided intellectual input. WT, XJ, and MRN conceived the study. WT and MRN wrote the manuscript.

*These authors contributed equally to this work.

Disclosures

Mark Nicolls and Wen Tian are co-inventors on the patent "Treatment of Pulmonary Hypertension with Leukotriene Inhibitors" to treat pulmonary hypertension" US2013251787A1. The other authors have no competing interests.

mediated pulmonary inflammation synergized with phenotypically-silent *Bmpr2* defects to elicit significant pulmonary vascular disease in rats.

Methods: Monoallelic *Bmpr2* mutant rats were generated and found phenotypically normal for up to one year of observation. To evaluate whether a second hit would elicit disease, animals were exposed to 5-LO-expressing adenovirus (Ad*Alox5*), monocrotaline, SU5416, SU5416 with chronic hypoxia or chronic hypoxia alone. *Bmpr2*-mutant hPAH patient samples were assessed for neointimal 5-LO expression. Pulmonary artery endothelial cells (PAECs) with impaired BMPR2 signaling were exposed to increased 5-LO-mediated inflammation and were assessed for phenotypic and transcriptomic changes.

Results: Lung inflammation, induced by intratracheal delivery of Ad*Alox5*, elicited severe PAH with intimal remodeling in *Bmpr2*$^{+/-}$ rats but not in their wild-type littermates. Neointimal lesions in the diseased *Bmpr2*$^{+/-}$ rats gained endogenous 5-LO expression associated with elevated LTB_4 biosynthesis. *Bmpr2-mutant* hPAH patients similarly expressed 5-LO in the neointimal cells. *In vitro*, BMPR2 deficiency, compounded by 5-LO-mediated inflammation, generated apoptosis-resistant, and proliferative PAECs with mesenchymal characteristics. These transformed cells expressed nuclear envelope-localized 5-LO consistent with induced LTB_4 production, as well as a transcriptomic signature similar to clinical disease, including upregulated NF-κB, IL-6, and TGF-β signaling pathways. The reversal of PAH and vasculopathy in *Bmpr2* mutants by TGF-β antagonism suggests that TGF-β is critical for neointimal transformation.

Conclusions: In a new ‘two-hit’ model of disease, lung inflammation induced severe PAH pathology in *Bmpr2*$^{+/-}$ rats. Endothelial transformation required the activation of canonical and noncanonical TGF-β signaling pathways and was characterized by 5-LO nuclear envelope translocation with enhanced LTB_4 production. This study offers one explanation of how an environmental injury unleashes the destructive potential of an otherwise-silent genetic mutation.

Keywords

lung; endothelial cells; *Bmpr2* insufficiency; inflammation

Introduction

While being the most common inherited risk factors for hPAH, *Bmpr2* germline mutations only result in disease in 20% of mutation carriers[1–3]; a finding that suggests a ‘second hit’ is required to elicit vascular pathology. Transgenic mouse models of *Bmpr2* mutations were developed to better understand the relationship between these phenotypically-silent gene mutations and the predisposition to PAH. Like 80% of human *Bmpr2* mutation carriers, most heterozygous *Bmpr2*- mutant mice and rats do not develop spontaneous PAH and enjoy a normal life span with an absence of lung pathology. However, a smaller subset of these animals develop some pulmonary vascular disease if the animals are allowed to age.[4,5] The acquired injury required to elicit significant pulmonary vascular remodeling and PAH in *Bmpr2* mutants is unknown. Understanding this process could help prevent disease in silent carriers.

Inflammation is a compelling candidate for the second signal causing fulminant PAH in phenotypically-normal gene mutants.[6] Our group has shown that vascular injury is

propagated by exaggerated inflammation caused by the absence of normal regulatory T cell (Treg) activityt86.[7–9] PAH patients demonstrate Treg abnormalities with evidence of systemic and lung immune activation.[10,11] In addition to derangements in T and B cell activity, innate immunity as manifested by enhanced neutrophil elastase and macrophage activation can participate in the pathogenesis of PAH.[9,12,13] IL-6 and TNF-α signaling inhibit BMPR2 signaling pathway and are implicated in preclinical and clinical PAH.[14,15] We found that macrophage-derived LTB_4, a 5-LO metabolite frequently observed in pulmonary inflammation[16], induces the apoptosis of PAECs, and the proliferation and activation of PA smooth muscle cells (PASMCs) and PA adventitial fibroblasts.[9,17] While a recent clinical PAH trial, specifically targeting LTB_4, did not achieve its primary endpoint (), there are several lines of evidence to suggest that 5-LO and the leukotrienes are relevant to the evolution of PAH.[18] Moreover, phenotypically-normal *Bmpr2* mutant mice exposed to 5-LO develop transiently elevated right ventricular systolic pressure (RVSP) for several days.[19] Given that 5-LO and LTB_4 are important components of inflammatory responses in lung injury, we questioned whether acquired pulmonary inflammation through this pathway could cause durable vascular remodeling in *Bmpr2* mutant rats.

Rat models of PAH are advantaged by high PA pressures and vascular remodeling not always achieved in mice.[20] We created two strains of monoallelic mutant rats with frameshift mutations in *Bmpr2* and found that these rats did not spontaneously develop pulmonary vascular pathology or PAH in the first year of life. We subsequently found that intratracheal administration of adenovirus-overexpressing *Alox5* (gene encoding 5-LO, Ad*Alox5*) caused severe PAH in both *Bmpr2* mutant strains with angioocclusive lesions, but left wild-type (WT) rats unaffected. By contrast, none of the other tested PAH-triggers differentiated *Bmpr2* mutant rats from WT animals, including monocrotaline (MCT), SU5416, SU5416 with chronic hypoxia or chronic hypoxia alone. In this new ‘two-hit’ model of disease, the *Alox5* transgene was administered in the large airways and generated pulmonary inflammation in the first week following its dosing. By week two, the diseased neointima began to autonomously synthesize nuclear envelope-localized 5-LO, which was non-viral in origin. The intimal 5-LO-expressing cells were also prominent in the pulmonary lesions of *Bmpr2*-mutant hPAH patients. *In vitro*, 5-LO-mediated inflammation similarly transformed PAECs into a diseased neointimal phenotype when BMPR2 signaling was diminished. The pathologically-transformed PAECs proliferated in the first three days in a noncanonical TGF-β signaling-dependent manner; after which, PAECs became increasingly inflamed and utilized canonical TGF-β signaling. Correspondingly, blocking TGF-β reversed PAH in *Bmpr2* mutant rats. In summary, this study provides a plausible ‘two-hit’ model of PAH that explains how phenotypically-silent *Bmpr2* mutations increase the susceptibility to inflammation-induced PAH by lowering the threshold for neointimal transformation.

Methods

All materials, datasets, and protocols used in this study will be made available to investigators upon request for the purpose of reproducing the results or replicating the procedure. Transcriptome data (FASTQ files) have been submitted to the Gene Expression Omnibus (GEO, GSE133749).

Animal Model

Construction of Bmpr2 mutant rats—Inbred F344 *Bmpr2* mutant rats were constructed using Zinc Finger Nuclease (ZFN) technology in the SAGE Laboratory. Two strains of rats, with monoallelic deletion of 527 bp *($Bmpr2^{+/\Delta 527bp}$*, Δ527 crosses intron and exon1 boundary) or 16bp *($Bmpr2^{+/\Delta 16bp}$*, Δ16 in exon1) resulting in frameshift mutation of *Bmpr2*, were developed in parallel. Both strains and both sexes were studied and compared to confirm the specific effects of *Bmpr2* haplodeficiency on the analyzed parameters (Supplemental Figure 1). WT rats were used as controls.

Delivery of 5-LO transgene—Full-length human 5-LO cDNA was cloned into an eGFP-tagged adenoviral vector harboring the CMV promotor by customer order in Vector Biolabs (Ad*Alox5*). Recombinant replication-deficient Ad*Alox5* (2.0×10^8 plaque-forming unit/animal) was introduced to the lung of the *Bmpr2* mutant or WT rats, 4–6-week-old, through intratracheal instillation. Subgroups of rats were treated with adenovirus-expressing eGFP control vector (Ad*GFP*) for comparison. All animals in the two-hit model were maintained in normoxic conditions. The experimental protocol was approved by the Veterans Affairs Palo Alto Animal Care and Use Committee.

Statistics—GraphPad Prism version 6.0c was used for statistical analysis. For comparisons between multiple experimental groups at a single time point, Kruskal-Wallis tests followed by Dunn's multiple comparisons tests for post-hoc analyses were used. For comparisons between two independent samples, Mann-Whitney tests were used. A p value of < 0.05 was considered significant. Detailed descriptions of hemodynamics measurement, echocardiography, immunohistochemistry, patient samples, human primary PAEC culture, shRNA infection, flow cytometry analysis, western blotting, real-time reverse transcription quantitative PCR (primer information provided in Supplemental Table 1), TGF-β reporter assays, data analysis and sample preparation of RNAseq are supplied in the online-only Data Supplement.

Results

Bmpr2 haploinsufficiency renders rats susceptible to inflammation-induced PAH.

To generate *Bmpr2* mutant rats, ZFN technology was used to target the *Bmpr2* gene to induce monoallelic deletion of 527bp *($Bmpr2^{+/\Delta 527bp}$)* or 16bp *($Bmpr2^{+/\Delta 16bp}$)* (Supplemental Figure 1). The *$Bmpr2^{+/\Delta 527bp}$* rats were first evaluated at 3, 6, 9 and 12 months of age for hemodynamic changes and RV remodeling and were phenotypically normal (Figure 1, A and B). The mutant rats were then assessed for increased responsiveness to several putative PAH triggers including intratracheal delivery of Ad*Alox5*, MCT, SU5416 and chronic hypoxia. Severe PAH was evident in *$Bmpr2^{+/\Delta 527bp}$* rats 3 weeks after Ad*Alox5* administration, with progressively increased RVSPs and RV/LV+S ratios over time (Figure 1, C and D and Supplemental Figure 2, A and B). Both female and male rats developed PAH with male rats exhibiting slightly higher RV hypertrophy (RVH) compared to their female cohort (Figure 1, E and F). The relatively high mortality of the mutant group exposed to Ad*Alox5* was attributable to declining RV function (Figure 1G and Supplemental Figure 2, C and D). Compatible with an acceptable model of PAH, left ventricular (LV) function was

preserved in the diseased rats (Supplemental Figure 2E). To correlate BMPR2 dysfunction with PAH pathogenesis, we examined the expression of BMPR2 and found that *Bmpr2*$^{+/-}$ rats with Ad*Alox5*-induced PAH experienced a reduction of whole lung BMPR2 protein (Figure 1, H and I). PAH in *Bmpr2*$^{+/\Delta 527bp}$ rats was characterized by enhanced muscularization of the distal pulmonary arteries and luminal obliteration (Figure 1, J and K). By contrast, none of the other PAH triggers tested, including MCT, SU5416 and/or chronic hypoxia, clearly differentiated *Bmpr2*$^{+/-}$ from WT rats, with the exception of heterozygous animals exposed to chronic hypoxia that showed a small increase in RVH (Supplemental Figure 3). We replicated these findings in the *Bmpr2*$^{+/\Delta 16bp}$ strain (Supplemental Figure 4). In summary, neither the single 'hit' of *Bmpr2* haploinsufficiency nor 5-LO-specific pulmonary inflammation causes disease, but their combined presence uniquely results in lethal PAH.

Bmpr2 mutant rats with PAH undergo extensive vascular remodeling.

Progressive vascular alterations lead to proliferative and occlusive neointima in preclinical and clinical PAH.2 To understand the relationship of time and neointimal remodeling in *Bmpr2*$^{+/-}$ rats experiencing evolving PAH, we assessed cleaved caspase 3 (apoptosis), Ki67 (proliferation) and α-SMA (vascular muscularization) in the Von Willebrand Factor positive (VWF+) vascular endothelium over time. Intimal cleaved caspase 3 expression was prominent 1 week following Ad*Alox5* instillation and gradually declined in *Bmpr2*$^{+/-}$ rats, confirming intimal injury as an early event of PAH in this model (Figure 2, A and B). Proliferating Ki67^{+} intimal cells increased over time and was concentrated in the neointima (Figure 2, C and D). Thickening of the α-SMA^{+} layer of distal PAs and intimal obliteration occurred after week 2 (Figure 2, E and F). α-SMA colocalized with vWF in the neointima at week 3 consistent with endothelial-to-mesenchymal transition (EndMT) in established PAH (Figure 2, E and F); EndMT is a pathological feature of preclinical and clinical PAH.[21–23]

Unresolved inflammation and dysregulated immunity underlie adverse PA remodeling, and 5-LO and its proinflammatory metabolite, LTB_4, have been implicated as effector molecules relevant to inflammatory PAH.[9,11,17] We found that the mutant rat lungs became progressively inflamed with increased numbers of perivascular macrophages (Supplemental Figure 5, A and B). Elevated whole lung transcription of *Il1r1* (interleukin-1 receptor 1), *Il6r, gp130* (glycoprotein 130, also known as IL-6Rβ), *Tlr2* (Toll-like receptor 2), *Tlr4* and *Gm-csf* (granulocyte-macrophage colony stimulating factor) further indicates heightened inflammation (Supplemental Figure 5, C and Supplemental Table 1). Perivascular 5-LO^{+} cells were notable in the first week (Figure 2G). At week 2, neointimal cells showed significant nuclear envelope 5-LO expression (Figure 2, G and H). 5-LO translocation to the nuclear envelope indicates active LTB_4 biosynthesis, a biological characteristic not observed in healthy endothelium (Supplemental Figure 5D).[24] Heightened pulmonary 5-LO expression was associated with elevated systemic LTB_4 concentrations (Supplemental Figure 5E). Congruent with several other experimental models of PAH[9], blocking LTB_4 beginning at week 3, reversed established disease by week 5 and prevented PAH-associated mortality; a finding indicating an important role of LTB_4 in this model (Supplemental Figure 5, F–H). In summary, *Bmpr2* mutant rats are susceptible to inflammation-induced PAH, in which vascular remodeling appears to be related to the gain of neointimal 5-LO.

Pulmonary inflammation leads to a neointima which expresses endogenous 5-LO.

We next sought to determine whether neointimal 5-LO expression was due to Ad*Alox5* infection or to an endogenous synthesis. GFP-tagged Ad*Alox5* transgene and its vector control (Ad*GFP*) were monitored over time in the *Bmpr2* mutant and WT rats following intratracheal instillation. In the first week, virus concentrated in the epithelial cells of conducting airways, alveoli and, to a lesser extent, alveolar macrophages; detection was diminished by week 2 and mostly absent by week 3 (Figure 2, I and J and Supplemental Figure 6, A–D). Ad*Alox5* distributed similarly in both *Bmpr2*$^{+/-}$ rats and WTs suggesting that the different responsiveness to Ad*Alox5* in the mutant and WT rats was attributable to the presence of the genetic mutation rather than differences in viral uptake (Supplemental Figure 6, A and B). Notably, neither Ad*Alox5* nor Ad*GFP* was detected in the pulmonary vasculature indicating that neointimal 5-LO expression was endogenous and not viral (Supplemental Figure 6, E and F). In other words, the increased 5-LO observed 3 weeks after Ad*Alox5* treatment was not derived from the original exogenous source but was instead owing to elevated endogenous expression. Immunoblotting of lung samples harvested at week 3 (when Ad*Alox5* was not present) showed an ≈5-fold increase in 5-LO expression in the diseased *Bmpr2*$^{+/-}$ rats (Supplemental Figure 6, G and H). In summary, to characterize this new two-hit model of PAH, we demonstrated that: 1) adenoviral-5LO first invades epithelial cells and alveolar macrophages, 2) viral transduction causes pulmonary inflammation and 3) recruits perivascular macrophages to produce LTB_4 (sufficient for PAEC apoptosis, PASMC expansion and adventitial fibroblast activation[9,17]), 4) the emergent neointima expresses endogenous, nuclear envelope-localized 5-LO consistent with active LTB_4 biosynthesis, and 5) as adenoviral 5-LO disappears from the lung, it is replaced by endogenous 5-LO which is sustained (Figure 2K).

hPAH neointima expresses 5-LO.

To determine whether neointimal 5-LO expression is also a clinical feature of hPAH harboring *Bmpr2* mutations, we evaluated 19 hPAH and 11 disease-control lungs (Supplemental Table 2 and 3). In vessels of different sizes from hPAH patients, 5-LO was expressed in the VWF+ neointima and localized on the nuclear envelope, whereas, endothelial 5-LO expression was nearly undetectable in control tissues (Figure 3, A and B). In a small clinical study, serum LTB_4 concentrations were also noted to be relatively elevated (Supplemental Figure 6I). Thus, like *Bmpr2*$^{+/-}$ rats with PAH, hPAH patients with *Bmpr2* mutations also develop a 5-LO expressing neointima that sustains vascular inflammation.

PAECs with compromised BMPR2 signaling exhibit a unique gene expression signature after exposure to Ad*Alox5*.

Given that these unique and clinically-relevant neointimal cells have not been well-described, we reasoned that a comprehensive transcriptome analysis by RNA sequence (RNAseq) could improve our understanding of the mechanisms underlying the intimal transformation. We performed RNAseq on human PAECs cultured with lentivirus expressing short hairpin RNA (shRNA) targeting *Bmpr2* (sh*Bmpr2*) and Ad*Alox5* to model the *in vivo* two-hit condition. These results were compared with PAECs treated with sh*Bmpr2* to model

cells from healthy mutants. Differential expression analysis between sh*Bmpr2*+Ad*Alox5* and sh*Bmpr2* groups showed a total of 403 up-regulated and 212 down-regulated differentially expressed genes (DEGs; Figure 3C, yellow circles; *FDR* = 0.05). To elucidate the unique gene expression signature of the two-hit model, we also performed analysis on sh*Bmpr2*-treatment groups versus sh*GFP* vector control groups and Ad*Alox5*-treatment groups (to model inflammation with conserved BMPR2 signaling) versus Ad*GFP* control groups (Figure 3C, Venn diagrams). The two-hit condition was associated with 335 uniquely up-regulated and 205 uniquely down-regulated genes which were distinct from the DEGs in the other two conditions (Figure 3C). Gene set enrichment analysis (GSEA) focusing on these DEGs revealed a number of significantly expressed genes that have been implicated in animal and human PAH.[25–27] Here, *CXCL8* and *CCL2* are associated with Hallmark geneset characteristics for IFN-γ responses; *NFKB1A, FAS, ALOX5, TLR2, TLR4 and IL1RL1* are associated with the geneset of TNF-α responses via NF-κB; *HIF1A* is associated with both the cell proliferation and the hypoxia and glycolysis responses; *TGFb1, TGFbR3, FN-1, PAI1, ITGA9*, and *HMGA1* belong to the epithelial-to-mesenchymal transition geneset (the same genes implicated in EndMT); and *STAT1* and *STAT3* belong to the IL-6/JAK/STAT3 geneset (Figure 3, C–E and Supplemental Figure 7). DEGs associated with cell proliferation responses, such as *HDAC1, FOXO1* and *EGFR* were presented in both the two-hit model and the Ad*Alox5* groups, confirming a pro-proliferative role of 5-LO-mediated inflammation (Figure 3, C–E and Supplemental Figure 7).[28,29] *IL-7R*, a potential biomarker for human disease[30], and *SMURF1*, a negative modulator of TGF-β signaling, were down-regulated only in the two-hit group (Figure 3, C and E and Supplemental Figure 7). In summary, PAECs with inhibited BMPR2 and heightened 5-LO immunity exhibit unique transcriptomic characteristics of inflammatory responses, EndMT, cell proliferation, and metabolism pathways already implicated in PAH.

PAECs exposed to impaired BMPR2 signaling and 5-LO-mediated inflammation become transformed.

We next determined the relationship between the phenotype of transformed PAECs and their transcriptome profile. Here, in addition to evaluating BMPR2 signaling loss in control PAECs treated with sh*Bmpr2*, we also assayed cells with endogenously compromised signaling (PAECs isolated from *Bmpr2* mutant hPAH lung). Perturbations of 5-LO-mediated immunity were tested by using LTB_4 at a concentration approximate to that of the BALF (bronchoalveolar lavage fluid) of PAH rats (400nM)[9]. LTB_4 reduced BMPR2 message, protein, and downstream canonical signaling (p-SMAD1/5/9, SMAD1, and Id-1; Supplemental Figure 8). These *in vitro* findings parallel the diminished BMPR2 expression observed *in vivo* (Figure 1, H and I). To determine whether PAECs with low BMPR2 signaling in high-[LTB_4] culture recapitulate progressive intimal remodeling *in vivo*, cellular apoptosis, proliferation, EndMT and endogenous 5-LO expression were examined over time respectively. Flow cytometry for cleaved caspase 3^+ cells indicates that LTB_4 induced apoptosis in ≈50% of PAECs within 24hrs, as published[9] (Supplemental Figure 9A). The surviving PAECs were proliferative and apoptosis-resistant after 3 days (Supplemental Figure 9, A and B). On day 7, these PAECs demonstrated further augmented proliferation and reduced apoptosis (Figure 4, A–F). Cell proliferation was confirmed by propidium iodide (PI)-mediated cell cycle analysis suggesting increased number of cells in the G2/M

phase on day 7 (Supplemental Figure 10). Some baseline α-SMA expression was observed in all groups on day 1 before any transformation had occurred. However, α-SMA expression was profoundly increased in the sh*Bmpr2*-treated PAECs 5 days after being cultured with LTB_4 (Supplemental Figure 9C). Additionally, PAECs with impaired BMPR2 signaling combined with LTB_4 displayed altered architecture; more of these cells lost the typical endothelial-specific cobblestone appearance and instead displayed an elongated mesenchymal-like spindle shape with fragmented VE-cadherin, a phenotype indicating compromised cell junctions (Figure 4, E, G and H).

To investigate whether BMPR2 deficiency and high [LTB_4] affect PAEC 5-LO expression as observed *in vivo*, immunofluorescent studies assessed intracellular 5-LO expression and its subcellular location. As previously reported[40], control PAECs did not express 5-LO (Figure 4, I and J). Significant nuclear 5-LO expression was observed in cells with low BMPR2 signaling (Figure 4, I and J). LTB_4 is metabolized very quickly ($T_{1/2}$≈90 seconds)[33], but we found that a single pulse of LTB_4 induced effects lasting >7 days. One week after addition of LTB_4, BMPR2-insufficient PAECs exhibited nucleoplasmic 5-LO translocation to the nuclear envelope and the ER/Golgi membrane, resulting in sustained LTB_4 synthesis (Figure 4, I–K). This LTB_4-producing inflammatory endothelial phenotype was further characterized by increased *Il1r1, Il6r, Tlr2*, and *Tlr4* transcripts in BMPR2-impaired PAECs, but not in cells with normal BMPR2 (Figure 4L and Supplemental Table 1). In conclusion, the presence of attenuated BMPR2 signaling increases the susceptibility of PAECs to undergo a progressive morphological and functional transformation after the exposure to LTB_4 (Figure 4M).

Attenuated BMPR2 signaling promotes PAEC TGF-β activation in high [LTB_4] conditions.

We used the RNAseq results to seek mechanistic explanations for why 5-LO-mediated inflammation negatively impacted PAECs with reduced BMPR2 signaling; to this end, we assessed TGF-β (SMAD-mediated canonical and p38-mediated noncanonical) pathways in this model. Abnormal canonical TGF-β signaling promotes endothelial dysfunction, EndMT and dysregulated immunity in PAH.[31,32,33] p38 signaling is important in both TGF-β signaling and 5-LO activation.[33,34] qPCR analysis demonstrated that LTB_4 induced *Pai1, Tgfb1* and *Itga9* transcription in BMPR2-low PAECs, all of which are TGF-β down-stream genes, significantly upregulated in the RNAseq results (Figure 5, A and C and Supplemental Table 1). We then used SBE (SMAD2/3 binding element) reporter assays to gauge TGF-β transcriptional activities in the same group of cells and found that LTB_4 significantly increased the TGF-β-induced luciferase gene expression (Figure 5, B and D). To address whether LTB_4 promoted both the SMAD-mediated canonical and the p38-mediated noncanonical TGF-β signaling in cells with BMPR2 defects, we assessed the protein expression of p-SMAD2/3, SMAD2/3, p-p38 and p38 and found increased activation of SMAD2/3 and p38 by LTB_4 (Figure 5, E–H). Immunofluorescent staining for p-SMAD2/3 and p-STAT3 (mediators of TGF-β/IL-6 effector pathway) showed intense expression in the obliterated center of PAs (Figure 5, I–L). These results collectively demonstrate that 5-LO-mediated inflammation may contribute to vascular remodeling via TGF-β signaling.

The apoptosis-resistance and increased proliferation of BMPR2-defective PAECs in high [LTB_4] conditions require p38-mediated noncanonical TGF-β signaling.

To more specifically assess how TGF-β signaling contributes to PAEC metamorphoses, treatment effects of inhibiting LTB_4 signaling (sh*Ltb4r1*, silencing the LTB_4 type 1 receptor, LTB_4R1) were compared to effects of antagonizing TGF-β receptor signaling, which attenuates both canonical and noncanonical TGF-β signaling (sh*Tgfβr1*, TGF-β receptor 1, TGFβR1). Further, to delineate the differential roles of canonical and p38-mediated noncanonical TGF-β signaling, sh*Smad3*, and a p38 blocker (SB203580) were tested simultaneously (Supplemental Figure 11). Treatments of sh*Ltb4r1*, sh*Tgfβr1*, or a p38 blocker normalized the aberrant, apoptosis-resistant proliferation in high [LTB_4] culture conditions (Figure 6, A–F and Supplemental Figure 12A). By contrast, canonical TGF-β antagonism (sh*Smad3*) was not effective (Figure 6, A–F and Supplemental Figure 12A). Cell cycle analysis confirmed these findings (Supplemental Figure 13). Together, these data demonstrate that the generation of apoptosis-resistant and proliferative PAECs requires the p38-dependent noncanonical TGF-β signaling pathway; a conclusion consistent with the requirement of this signaling for abnormal cell survival and proliferation[35]

EndMT, observed in BMPR2-low/[LTB_4]-high conditions, requires canonical TGF-β signaling.

SMAD2/3-mediated canonical TGF-β is implicated in PAEC EndMT *in vitro*[21,22] Here, we tested the importance of canonical TGF-β signaling for the mesenchymal cell-like phenotype. Strategies that blocked LTB_4 (sh*Ltb4r1*) or inhibited canonical TGF-β signaling (sh*Tgfβr1* or sh*Smad3*) abolished hPAH-PAEC spindle cell morphology, restored cellular junctions, attenuated α-SMA expression, reduced *Calponin, Snail, Slug* mRNA transcription and normalized *Ve-cadherin* (Figure 6, E, G and H, Supplemental Figures 12B and 14, and Supplemental Table 1). By contrast, blocking p38-mediated noncanonical TGF-β signaling did not affect EndMT (Figure 6, E, G and H and Supplemental Figures 12 and 14). Cumulatively, these results indicate that the evolution of a mesenchymal phenotype in this model requires canonical TGF-β signaling.

TGF-β signaling is required for inflammatory endothelial phenotype.

PAECs and the neointima in the current model are remarkable for increased nuclear envelope 5-LO, LTB_4 biosynthesis and other inflammatory mediators. Given the demonstrated relationship between noncanonical and canonical TGF-β signaling, we evaluated how these pathways related to the inflammatory parameters observed in culture. Blocking either canonical and/or noncanonical TGF-β signaling prevented translocation of 5-LO in the PAEC nuclei, thus attenuating endothelial LTB_4 biosynthesis (Figure 6, I–K). Additionally, blocking TGF-β reversed IL-1, IL-6 or TLR-mediated vascular inflammation (Figure 6L and Supplemental Table 1). Collectively, the cumulative results demonstrate that the inflammatory phenotype of the transformed PAECs requires TGF-β signaling.

Blocking TGF-β signaling attenuates 5-LO-induced PAH in the *Bmpr2* mutant rats.

Based on the *in vitro* findings, we sought to determine whether inhibiting TGF-β receptor signaling, an approach attenuating both canonical and noncanonical pathways, would be

beneficial to *Bmpr2*$^{+/-}$ rats with 5-LO-induced PAH. SB431542, a potent, selective inhibitor of TGFβR1 (also named as activin receptor-like kinase 5, ALK5) was chosen for this purpose and has demonstrated efficacy in the preclinical *Schistosoma*-induced, chronic hypoxia or MCT model of PAH.[36,37] In a protocol in which SB431542 was commenced 3 weeks following Ad*Alox5* (a time point when PAH was already advanced), 2 weeks of daily treatment with SB431542 attenuated PAH, reduced intimal SMAD2/3 activation, diminished vascular remodeling, reversed the angioproliferation of intimal cells, and abrogated neointimal 5-LO expression (Figure 7). These data collectively suggest that TGF-β signaling plays a critical role in the two-hit disease process of intimal remodeling prompted by *Bmpr2* haploinsufficiency and 5-LO-mediated pulmonary inflammation.

Discussion

This study adds to a growing knowledge base that addresses how *Bmpr2* mutations place individuals at risk for a life-threatening cardiopulmonary disease. Compared to idiopathic PAH patients, *Bmpr2* mutant patients exhibit a more severe PAH phenotype and suffer worse outcomes.[38,39] Here, we demonstrated that *Bmpr2* mutant rats developed severe PAH with extensive vascular remodeling and high mortality when exposed to 5-LO-mediated lung inflammation. This is a two-hit model because *Bmpr2* mutations were phenotypically-silent and 5-LO-mediated inflammation alone produced no PAH. The *Bmpr2*$^{+/-}$ rats with PAH exhibited a transformed neointima characterized by proliferative cells with non-viral 5-LO expression, attributes shared by hPAH lungs. PAECs with impaired BMPR2 signaling, when exposed to the 5-LO metabolite, LTB_4, similarly resulted in an apoptosis-resistant, proliferative and mesenchymal cell-like phenotype, capable of self-sustained inflammation. Additionally, this study identified a novel mechanism by which 5-LO-mediated inflammation enhanced canonical and noncanonical TGF-β signaling to promote PAEC transformation (Figure 8).

Unlike the current study, a recent investigation of transgenic *Bmpr2*$^{+/-}$ rats showed age-dependent spontaneous PAH in 20% of carrierst.[5] Study differences may reflect dissimilar genetic backgrounds, diets, and housing conditions. Spontaneous PAH in the prior model did not occur in females and was relatively mild.[5] In the current study, both female and male mutant rats developed severe PAH after exposure of Ad*Alox5*, with male rats exhibiting greater RV hypertrophy; a finding similar to clinical disease in which females are more susceptible to disease but more severe when present in males.[40] Prior *Bmpr2* mutant PAH models suggested that a ‘second hit’ might be required to elicit vascular pathology[41] Ad*Alox5* induces a transient elevation in RVSP and mild vascular muscularization in *Bmpr2*$^{+/-}$ mice[19] with RVSP peaking at day seven and returning to normal by day 21. In this respect, the differences between transgenic mice and rats may be attributable to rats developing a 5-LO-expressing inflammatory neointima. Analogous to a lung infection causing acute respiratory distress syndrome (ARDS), Ad*Alox5* triggered sustained vascular inflammation.

5-LO activity depends on its subcellular compartmentalization, phosphorylation state and proximity to other eicosanoid-forming enzymes.[16,24] Cytosolic 5-LO expression is not observed in healthy PAECs by standard biochemical measures[40,41], but is detected after

culture with LTB_4. BMPR2-inhibited PAECs displayed increased nucleoplasmic 5-LO. Addition of LTB_4 to these BMPR2-inhibited cells translocated the nuclear 5-LO to the envelope margin where LTB_4 production occurs (i.e., exogenous LTB_4 promoted endogenous LTB_4). Healthy PAECs don't express 5-LO possibly because the methylation of the *Alox5* promoter at CpG residues normally suppresses its transcription.[42] Engagement of NF-κB, SMAD2/3 or TGF-β responsive element on the *Alox5* promoter may profoundly induce *Alox5*[43] Collectively considered, heightened inflammation with activated TGF-β signaling in PAECs may give rise to pronounced 5-LO expression when BMPR2 signaling is compromised.

Transformed PAECs in this study were more proliferative and inflamed, similar to the PAECs isolated from preclinical and clinical PAH lungs.[11,44] Decreased BMPR2 signaling creates a proclivity to PAEC apoptosis.[45] However, the mechanism by which BMPR2 deficiency potentiates apoptosis-resistant proliferation *in vivo* is not well understood. 5-LO signaling has been previously implicated as a mediator for the growth of PAECs, cancer cells and stem cells[28,29] and may play a role in the proliferative responses of neointima. The proliferative role of 5-LO is consistent with our finding that LTB_4 alone also induced apoptosis-resistant proliferation of BMPR2-conserved PAECs without further pathological alterations. Accordingly, Ad*Alox5* did not induce PAH in the WT rats; a fact that was central to the logic of the two-hit model. However, LTB_4 did induce early pathology in cultured PAECs with normal BMPR2. The apparent discrepancy between 5-LO immunity on animals and on cultured cells may be a function of the time points examined (i.e., *in vivo* pathology was examined at 3 weeks while *in vitro* studies primarily evaluated cultures in the first week); an earlier examination of cardiopulmonary tissue may show transient pathology in WT rats receiving Ad*Alox5*. We postulate that a BMPR2-conserved PA endothelium employs a reparative mechanism such that LTB_4-mediated injury does not cause disease. With BMPR2-insufficiency, the unique two-hit conditions are present to favor PAEC transformation. These findings are comparable in a way to the SU5416/hypoxia 2-hit model of PAH, where SU5416 alone causes PAEC death without PAH.[46]

Why 5-LO-mediated inflammation promoted SMAD2/3 is unknown. One possibility is that LTB_4 may increase the bioavailability of TGF-β1 for its cognate receptor, and high [TGFβ1] favors the increased expression of SMAD2/3.[47] This hypothesis is supported by increased TGFβ1, LTBP-1 (latent TGF-β-binding protein) and TGFβR3 transcription in the BMPR2-low/5-LO-high PAECs. 5-LO may also act as a transcriptional modulator[48,49] to augment SMAD2 while suppressing SMAD1 and SMAD9 transcripts. We did not investigate SMAD2 signaling in the current study, because SMAD3, but not SMAD2 is implicated in vascular remodeling of Schistosoma-induced and hypoxia-induced PAH models[36] Collectively, our study expands the established concepts of PAEC EndMT by showing how BMPR2 signaling deficiency compounds a discrete inflammatory injury to generate a transformed endothelium via canonical and noncanonical TGF-β signaling.

A recent clinical trial () failed to demonstrate the efficacy of targeting LTB_4 for PAH. The current study suggests that eicosanoid mediators of inflammation may be particularly relevant in patients with BMPR2 mutations, a subset not specifically enrolled in this clinical study. In addition to this possibility, other explanations for the failure of LTB_4 antagonism to

reverse clinical disease in all PAH patients include: 1) drug-drug interactions (all enrolled patients were on at least one vasodilator therapy), 2) 5-LO-related immunity is less relevant to disease maintenance as it appears to be for disease pathogenesis, and 3) patients enrolled had heterogeneous causes of PAH for which 5-LO-related immunity was not consistently relevant. As with other inflammatory diseases, it is becoming increasingly apparent that disease biomarkers, such as BMPR2 mutations, should be evaluated prospectively to discern which patients will most benefit from targeted immune modulation.

This study had several limitations. While we elected to focus on the endothelium because of our prior work showing that LTB_4 is toxic to PAECs and because of the intimal remodeling observed in our animal models,[9,17] our prior studies also demonstrate that LTB_4 directly affects PASMCs and PA adventitial fibroblasts. Additional mechanisms of disease evolution likely involve these other cell types in the two-hit model of PAH. To discern which cell populations contribute to the creation of neointimal cells, careful lineage fate-mapping studies are required and are currently limited to mouse models of disease (e.g.,[23]). Further, we used *in vitro* studies to explain how inflammation could complicate EndMT in BMPR2-reduced PAECs. However, *in vitro* cell-culture techniques have inherent limitations, such as stressful culture conditions, which can affect cellular behavior.[48,49] For example, we observed a baseline expression of α-SM A in ≈ 20% of cultured PAECs after 24 hours of culture even though, in other respects, these cells had not undergone EndMT; regardless, different experimental interventions led to clearly different outcomes that reflected intimal changes in the rat model of disease. Further, silencing of BMPR2 signaling with sh*Bmpr2* is not equivalent to BMPR2 haploinsufficiency; fortunately, our analyses with hPAH PAECs yielded similar results. Finally, we found that antagonizing SMAD3 or p38 signaling in PAECs prevented inflammation, suggesting that both the canonical and non-canonical TGF-β pathways are mediators of endothelial transformation. However, because p38 has pleiotropic roles, including the phosphorylation of 5-LO[34,35], an important caveat is that the anti-inflammatory effects of p38 inhibition may also be attributable to blocking 5-LO activation. The two-hit model of PAH provides a useful platform for future studies that can address other relevant target cell populations, human PAEC culture conditions, and p38 function.

In summary, *Bmpr2*-haploinsufficient individuals are at significant risk for PAH; there a significant need to understand how acquired factors, like inflammation, can elicit disease. We discovered that, following lung inflammation, 5-LO and its metabolite, LTB_4, working through TGF-β pathway activation synergized with phenotypically-silent *Bmpr2* mutations to cause endothelial transformation. Limiting pulmonary inflammation in patients with a genetic risk for PAH may prevent the development of serious cardiopulmonary disease.

Supplementary Material

Refer to Web version on PubMed Central for supplementary material.

Acknowledgments

We thank the SAGE laboratory for constructing the *Bmpr2* mutant rats. We acknowledged the Genome Sequencing Service at Center for Genomics and Personalized Medicine at Stanford University for RNAseq and data analysis.

Sources of Funding

This study was supported by NIH grant HL014985, HL122887, and HL138473 to M.R. Nicolls. XJ was partially supported by K12 training grant HL120001. RNAseq and data analysis was supported by NIH grant S10OD020141. Additional funding provided by a Vera Moulton Wall Center Seed Grant.

Non-standard Abbreviations and Acronyms:

BMPR2	Bone Morphogenic Protein Receptor 2
hPAH	hereditary pulmonary arterial hypertension
5-LO	5-lipoxygenase
LTB_4	Leukotriene B_4
Ad*Alox5*	5-lipoxygenase-expressing adenovirus
PAEC	pulmonary artery endothelial cell
Treg	regulatory T cell
PASMC	pulmonary artery smooth muscle cell
RVSP	right ventricular systolic pressure
Alox5	gene encoding 5-lipoxygenase
WT	wild-type
MCT	monocrotaline
ZFN	Zinc Finger Nuclease
***Bmpr2*$^{+/\Delta 527bp}$**	Bmpr2 mutation with monoallelic deletion of 527 bp
***Bmpr2*$^{+/\Delta 16bp}$**	Bmpr2 mutation with monoallelic deletion of 16 bp
Ad*GFP*	eGFP-expressing adenovirus
RV/LV+S	right ventricle / left ventricle + septum ratio
α-SMA	α smooth muscle actin
vWF	Von Willebrand Factor
RNAseq	RNA sequence
sh*Bmpr2*	lentivirus expressing short hairpin RNA targeting *Bmpr2*
ARDS	acute respiratory distress syndrome

References

1. Newman JH, Wheeler L, Lane KB, Loyd E, Gaddipati R, Phillips JA 3rd and Loyd JE. Mutation in the gene for bone morphogenetic protein receptor II as a cause of primary pulmonary hypertension in a large kindred. N E ngl J Med. 2001;345:319–324.

2. Humbert M, Guignabert C, Bonnet S, Dorfmuller P, Klinger JR, Nicolls MR, Olschewski AJ, Pullamsetti SS, Schermuly RT, Stenmark KR and Rabinovitch M. Pathology and pathobiology of pulmonary hypertension: state of the art and research perspectives. Eur Respir J. 2019;53: pii: 1801887. doi: 10.1183/13993003.01887-2018.

3. Morrell NW, Aldred MA, Chung WK, Elliott CG, Nichols WC, Soubrier F, Trembath RC and Loyd JE. Genetics and genomics of pulmonary arterial hypertension. Eur Respir J. 2019;53: pii: 1801899. doi: 10.1183/13993003.01899-201.

4. Long L, Ormiston ML, Yang X, Southwood M, Graf S, Machado RD, Mueller M, Kinzel B, Yung LM, Wilkinson JM, Moore SD, Drake KM, Aldred MA, Yu PB, Upton PD and Morrell NW. Selective enhancement of endothelial BMPR-II with BMP9 reverses pulmonary arterial hypertension. Nat Med. 2015;21:777–785. [PubMed: 26076038]

5. Hautefort A, Mendes-Ferreira P, Sabourin J, Manaud G, Bertero T, Rucker-Martin C, Riou M, Adao R, Manoury B, Lambert M, Boet A, Lecerf F, Domergue V, Bras-Silva C, Gomez AM, Montani D, Girerd B, Humbert M, Antigny F and Perros F. Bmpr2 Mutant Rats Develop Pulmonary and Cardiac Characteristics of Pulmonary Arterial Hypertension. Circu/ation. 2019;139:932–948.

6. Perros F, Dorfmuller P, Montani D, Hammad H, Waelput W, Girerd B, Raymond N, Mercier O, Mussot S, Cohen-Kaminsky S, Humbert M and Lambrecht BN. Pulmonary lymphoid neogenesis in idiopathic pulmonary arterial hypertension. Am J Respir Crit Care Med. 2012;185:311–321. [PubMed: 22108206]

7. Tamosiuniene R, Manouvakhova O, Mesange P, Saito T, Qian J, Sanyal M, Lin YC, Nguyen LP, Luria A, Tu AB, Sante JM, Rabinovitch M, Fitzgerald DJ, Graham BB, Habtezion A, Voelkel NF, Aurelian L and Nicolls MR. Dominant Role for Regulatory T Cells in Protecting Females Against Pulmonary Hypertension. Circ Res. 2018;122:1689–1702. [PubMed: 29545367]

8. Tamosiuniene R, Tian W, Dhillon G, Wang L, Sung YK, Gera L, Patterson AJ, Agrawal R, Rabinovitch M, Ambler K, Long CS, Voelkel NF and Nicolls MR. Regulatory T cells limit vascular endothelial injury and prevent pulmonary hypertension. Circ Res. 2011;109:867–879. [PubMed: 21868697]

9. Tian W, Jiang X, Tamosiuniene R, Sung YK, Qian J, Dhillon G, Gera L, Farkas L, Rabinovitch M, Zamanian RT, Inayathullah M, Fridlib M, Rajadas J, Peters-Golden M, Voelkel NF and Nicolls MR. Blocking macrophage leukotriene b4 prevents endothelial injury and reverses pulmonary hypertension. Sci Trans/Med. 2013;5:200ra117.

10. Tamosiuniene R and Nicolls MR. Regulatory T cells and pulmonary hypertension. Trends Cardiovasc Med. 2011;21:166–171. [PubMed: 22814424]

11. Rabinovitch M, Guignabert C, Humbert M and Nicolls MR. Inflammation and immunity in the pathogenesis of pulmonary arterial hypertension. Circ Res. 2014;115:165–175. [PubMed: 24951765]

12. Nickel NP, Spiekerkoetter E, Gu M, Li CG, Li H, Kaschwich M, Diebold I, Hennigs JK, Kim KY, Miyagawa K, Wang L, Cao A, Sa S, Jiang X, Stockstill RW, Nicolls MR, Zamanian RT, Bland RD and Rabinovitch M. Elafin Reverses Pulmonary Hypertension via Caveolin-1- Dependent Bone Morphogenetic Protein Signaling. Am J Respir Crit Care Med. 2015;191:1273–1286. [PubMed: 25853696]

13. Sawada H, Saito T, Nickel NP, Alastalo TP, Glotzbach JP, Chan R, Haghighat L, Fuchs G, Januszyk M, Cao A, Lai YJ, Perez Vde J, Kim YM, Wang L, Chen PI, Spiekerkoetter E, Mitani Y, Gurtner GC, Sarnow P and Rabinovitch M. Reduced BMPR2 expression induces GM-CSF translation and macrophage recruitment in humans and mice to exacerbate pulmonary hypertension. J Exp Med. 2014;211:263–280. [PubMed: 24446489]

14. Brock M, Trenkmann M, Gay RE, Michel BA, Gay S, Fischler M, Ulrich S, Speich R and Huber LC. Interleukin-6 modulates the expression of the bone morphogenic protein receptor type II through a novel STAT3-microRNA cluster 17/92 pathway. Circ Res. 2009;104:1184–1191. [PubMed: 19390056]

15. Li L, Wei C, Kim IK, Janssen-Heininger Y and Gupta S. Inhibition of nuclear factor-kappaB in the lungs prevents monocrotaline-induced pulmonary hypertension in mice. Hypertension. 2014;63:1260–1269. [PubMed: 24614212]

16. Peters-Golden M and Henderson WR Jr. Leukotrienes. N Engl J Med. 2007;357:1841–1854. [PubMed: 17978293]

17. Qian J, Tian W, Jiang X, Tamosiuniene R, Sung YK, Shuffle EM, Tu AB, Valenzuela A, Jiang S, Zamanian RT, Fiorentino DF, Voelkel NF, Peters-Golden M, Stenmark KR, Chung L, Rabinovitch M and Nicolls MR. Leukotriene B4 Activates Pulmonary Artery Adventitial Fibroblasts in Pulmonary Hypertension. Hypertension. 2015;66:1227–1239. [PubMed: 26558820]

18. Wright L, Tuder RM, Wang J, Cool CD, Lepley RA and Voelkel NF. 5-Lipoxygenase and 5-lipoxygenase activating protein (FLAP) immunoreactivity in lungs from patients with primary pulmonary hypertension. Am J Respir Crit Care Med. 1998;157:219–229. [PubMed: 9445303]

19. Song Y, Jones JE, Beppu H, Keaney JF Jr., Loscalzo J and Zhang YY. Increased susceptibility to pulmonary hypertension in heterozygous BMPR2-mutant mice. Circulation. 2005;112:553–562. [PubMed: 16027259]

20. Gomez-Arroyo J, Saleem SJ, Mizuno S, Syed AA, Bogaard HJ, Abbate A, Taraseviciene- Stewart L, Sung Y, Kraskauskas D, Farkas D, Conrad DH, Nicolls MR and Voelkel NF. A brief overview of mouse models of pulmonary arterial hypertension: problems and prospects. Am J Physiol Lung Cell M ol Physiol. 2012;302:L977–991.

21. Hopper RK, Moonen JR, Diebold I, Cao A, Rhodes CJ, Tojais NF, Hennigs JK, Gu M, Wang L and Rabinovitch M. In Pulmonary Arterial Hypertension, Reduced BMPR2 Promotes Endothelial-to-Mesenchymal Transition via HMGA1 and Its Target Slug. Circulation. 2016;133:1783–1794. [PubMed: 27045138]

22. Ranchoux B, Antigny F, Rucker-Martin C, Hautefort A, Pechoux C, Bogaard HJ, Dorfmuller P, Remy S, Lecerf F, Plante S, Chat S, Fadel E, Houssaini A, Anegon I, Adnot S, Simonneau G, Humbert M, Cohen-Kaminsky S and Perros F. Endothelial-to-mesenchymal transition in pulmonary hypertension. Circulation. 2015;131:1006–1018. [PubMed: 25593290]

23. Qiao L, Nishimura T, Shi L, Sessions D, Thrasher A, Trudell JR, Berry GJ, Pearl RG and Kao PN. Endothelial fate mapping in mice with pulmonary hypertension. Circulation. 2014;129:692–703. [PubMed: 24201301]

24. Luo M, Jones SM, Peters-Golden M and Brock TG. Nuclear localization of 5-lipoxygenase as a determinant of leukotriene B4 synthetic capacity. Proc Natl Acad Sci U S A. 2003;100:12165–12170. [PubMed: 14530386]

25. Rhodes CJ, Im H, Cao A, Hennigs JK, Wang L, Sa S, Chen PI, Nickel NP, Miyagawa K, Hopper RK, Tojais NF, Li CG, Gu M, Spiekerkoetter E, Xian Z, Chen R, Zhao M, Kaschwich M, Del Rosario PA, Bernstein D, Zamanian RT, Wu JC, Snyder MP and Rabinovitch M. RNA Sequencing Analysis Detection of a Novel Pathway of Endothelial Dysfunction in Pulmonary Arterial Hypertension. Am J Respir Crit Care Med. 2015;192:356–366. [PubMed: 26030479]

26. Stearman RS, Bui QM, Speyer G, Handen A, Cornelius AR, Graham BB, Kim S, Mickler EA, Tuder RM, Chan SY and Geraci MW. Systems Analysis of the Human Pulmonary Arterial Hypertension Lung Transcriptome. Am J Respir Cell M ol Biol. 2018.

27. Savai R, Al-Tamari HM, Sedding D, Kojonazarov B, Muecke C, Teske R, Capecchi MR, Weissmann N, Grimminger F, Seeger W, Schermuly RT and Pullamsetti SS. Pro-proliferative and inflammatory signaling converge on FoxO1 transcription factor in pulmonary hypertension. Nat Med. 2014;20:1289–1300. [PubMed: 25344740]

28. Walker JL, Loscalzo J and Zhang YY. 5-Lipoxygenase and human pulmonary artery endothelial cell proliferation. Am J Physiol Heart Circ Physiol. 2002;282:H585–593. [PubMed: 11788406]

29. Steinhilber D, Fischer AS, Metzner J, Steinbrink SD, Roos J, Ruthardt M and Maier TJ. 5-lipoxygenase: underappreciated role of a pro-inflammatory enzyme in tumorigenesis. Front Pharmacol. 2010;1:143. [PubMed: 21833182]

30. Risbano MG, Meadows CA, Coldren CD, Jenkins TJ, Edwards MG, Collier D, Huber W, Mack DG, Fontenot AP, Geraci MW and Bull TM. Altered immune phenotype in peripheral blood cells of patients with scleroderma-associated pulmonary hypertension. Clin Transl Sci. 2010;3:210–218. [PubMed: 20973920]

31. Akhurst RJ and Hata A. Targeting the TGFbeta signalling pathway in disease. Nat Rev Drug Discov. 2012;11:790–811. [PubMed: 23000686]

32. Medici D, Potenta S and Kalluri R. Transforming growth factor-beta2 promotes Snail-mediated endothelial-mesenchymal transition through convergence of Smad-dependent and Smad-independent signalling. Biochem J. 2011;437:515–520. [PubMed: 21585337]

33. Massague J TGFbeta signalling in context. Nat Rev Mol Cell Biol. 2012;13:616–630. [PubMed: 22992590]
34. Werz O, Klemm J, Samuelsson B and Radmark O. 5-lipoxygenase is phosphorylated by p38 kinase-dependent MAPKAP kinases. Proc Natl Acad Sci U S A. 2000;97:5261–5266. [PubMed: 10779545]
35. Sharma GD, He J and Bazan HE. p38 and ERK1/2 coordinate cellular migration and proliferation in epithelial wound healing: evidence of cross-talk activation between MAP kinase cascades. J Biol Chem. 2003;278:21989–21997. [PubMed: 12663671]
36. Graham BB, Chabon J, Gebreab L, Poole J, Debella E, Davis L, Tanaka T, Sanders L, Dropcho N, Bandeira A, Vandivier RW, Champion HC, Butrous G, Wang XJ, Wynn TA and Tuder RM. Transforming growth factor-beta signaling promotes pulmonary hypertension caused by Schistosoma mansoni. Circulation. 2013;128:1354–1364. [PubMed: 23958565]
37. Ma W, Han W, Greer PA, Tuder RM, Toque HA, Wang KK, Caldwell RW and Su Y. Calpain mediates pulmonary vascular remodeling in rodent models of pulmonary hypertension, and its inhibition attenuates pathologic features of disease. J Clin Invest. 2011;121:4548–4566. [PubMed: 22005303]
38. Larkin EK, Newman JH, Austin ED, Hemnes AR, Wheeler L, Robbins IM, West JD, Phillips JA 3rd, Hamid R and Loyd JE. Longitudinal analysis casts doubt on the presence of genetic anticipation in heritable pulmonary arterial hypertension. Am J Respir Crit Care Med. 2012;186:892–896. [PubMed: 22923661]
39. Evans JD, Girerd B, Montani D, Wang XJ, Galie N, Austin ED, Elliott G, Asano K, Grunig E, Yan Y, Jing ZC, Manes A, Palazzini M, Wheeler LA, Nakayama I, Satoh T, Eichstaedt C, Hinderhofer K, Wolf M, Rosenzweig EB, Chung WK, Soubrier F, Simonneau G, Sitbon O, Graf S, Kaptoge S, Di Angelantonio E, Humbert M and Morrell NW. BMPR2 mutations and survival in pulmonary arterial hypertension: an individual participant data meta-analysis. Lancet Respir Med. 2016;4:129–137. [PubMed: 26795434]
40. Humbert M, Guignabert C, Bonnet S, Dorfmuller P, Klinger JR, Nicolls MR, Olschewski AJ, Pullamsetti SS, Schermuly RT, Stenmark KR and Rabinovitch M. Pathology and pathobiology of pulmonary hypertension: state of the art and research perspectives. Eur Respir J. 2018.
41. Long L, MacLean MR, Jeffery TK, Morecroft I, Yang X, Rudarakanchana N, Southwood M, James V, Trembath RC and Morrell NW. Serotonin increases susceptibility to pulmonary hypertension in BMPR2-deficient mice. Circ Res. 2006;98:818–827. [PubMed: 16497988]
42. Radmark O and Samuelsson B. 5-Lipoxygenase: mechanisms of regulation. J Lipid Res. 2009;50 Suppl:S40–45. [PubMed: 18987389]
43. Seuter S, Sorg BL and Steinhilber D. The coding sequence mediates induction of 5-lipoxygenase expression by Smads3/4. Biochem Biophys Res Commun. 2006;348:1403–1410. [PubMed: 16919603]
44. Sweatt AJ, Hedlin HK, Balasubramanian V, Hsi A, Blum LK, Robinson WH, Haddad F, Hickey PM, Condliffe R, Lawrie A, Nicolls MR, Rabinovitch M, Khatri P and Zamanian RT. Discovery of Distinct Immune Phenotypes Using Machine Learning in Pulmonary Arterial Hypertension. Circ Res. 2019;124:904–919. [PubMed: 30661465]
45. Teichert-Kuliszewska K, Kutryk MJ, Kuliszewski MA, Karoubi G, Courtman DW,Zucco L, Granton J and Stewart DJ. Bone morphogenetic protein receptor-2 signaling promotes pulmonary arterial endothelial cell survival: implications for loss-of-function mutations in the pathogenesis of pulmonary hypertension. Circ Res. 2006;98:209–217. [PubMed: 16357305]
46. Taraseviciene-Stewart L, Kasahara Y, Alger L, Hirth P, Mc Mahon G, Waltenberger J, Voelkel NF and Tuder RM. Inhibition of the VEGF receptor 2 combined with chronic hypoxia causes cell death-dependent pulmonary endothelial cell proliferation and severe pulmonary hypertension. The FASEB journal: official publication of the Federation of American Societies for Experimental Biology. 2001;15:427–438. [PubMed: 11156958]
47. Brown KA, Pietenpol JA and Moses HL. A tale of two proteins: differential roles and regulation of Smad2 and Smad3 in TGF-beta signaling. J Cell Biochem. 2007;101:9–33. [PubMed: 17340614]
48. Skardal A, Mack D, Atala A and Soker S. Substrate elasticity controls cell proliferation, surface marker expression and motile phenotype in amniotic fluid-derived stem cells. J Mech Behav Biomed Mater. 2013;17:307–316. [PubMed: 23122714]

49. Mangum LH, Natesan S, Stone R 2nd, Wrice NL, Larson DA, Florell KF, Christy BA, Herzig MC, Cap AP and Christy RJ. Tissue Source and Cell Expansion Condition Influence Phenotypic Changes of Adipose-Derived Stem Cells. Stem Cells Int. 2017;2017:7108458. [PubMed: 29138638]

Clinical Perspective

What is new?

- In a new 'two-hit' model of disease, *Bmpr2* mutant rats, subjected to pulmonary inflammation, develop severe PAH with vascular remodeling.
- 5-LO-expressing neointimal lesions in *Bmpr2* mutant rats and patients may promote persistent vascular inflammation.
- Reducing PAEC BMPR2 signaling and enhancing 5-LO-mediated inflammation generate proliferative, inflammatory, and mesenchymal cells.
- PAEC transformation occurs in three phases: an initial apoptosis phase induced by exogenous LTB_4; a proliferative phase relying on p38-mediated noncanonical TGF-β signaling; and finally, a terminal inflammatory phase, in which PAECs utilize the canonical TGF-β pathway, express mesenchymal markers, and produce LTB_4, IL-6, and NF-κB signaling molecules.

What are the clinical implications?

- In phenotypically-silent *Bmpr2* haploinsufficient individuals, a second hit of pulmonary inflammation may put them at risk of developing PAH.
- Lung inflammation, while usually self-limited, may cause durable and inflammatory pulmonary vascular lesions in genetically-susceptible patients.

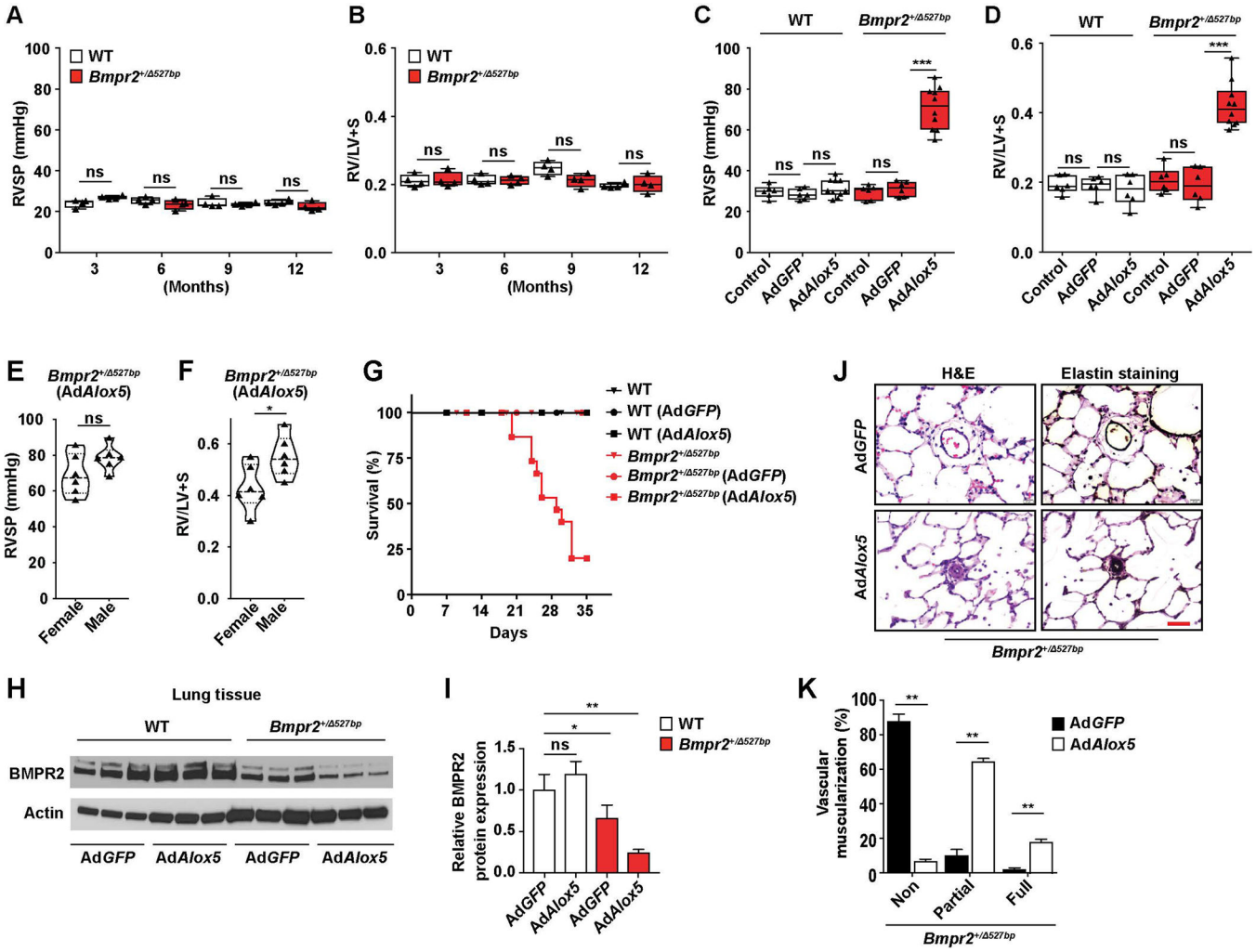

Figure 1. *Bmpr2* haploinsuffiriency renders rats susceptible to PAH following 5-LO-mediated pulmonary inflammation.

(**A** and **B**) Assessments of right ventricular systolic pressure (RVSP, **A**) and right ventricular hypertrophy ((weight ratio of right ventricle (RV) to left ventricle (LV) plus septum (S), RV/LV+S, **B**)) of *Bmpr2*$^{+/\Delta 527bp}$ rats at the 3, 6, 9 or 12 months of age. Hemodynamics measurements of WT cohort in the same age groups were analyzed in parallel. (**C**–**G**) Assessments of RVSP (**C**), RV/LV+S (**D**) and percentage of survival (**G**) of WT or *Bmpr2*$^{+/394527bp}$ rats administered with intratracheal instillation of adenovirus overexpressing *Alox5* (gene encoding for 5-LO, Ad*Alox5)* or GFP-tagged control vector (Ad*GFP*). Rats not subjected to virus treatments were used as controls. Hemodynamics measurements were performed at post-operative week 3. Female and male rats were randomly assigned to different experimental groups and compared (**E** and **F**). (**H** and **I**) Representative western blots and quantification of BMPR2 in lung tissue collected from WT and *Bmpr2*$^{+/\Delta 527bp}$ rats assigned in different treatment groups at post-operative week 3. Actin was used as loading control. n=3. (**J** and **K**) Representative hematoxylin and eosin (H&E) and Elastin stain images and quantification of percentage vascular muscularization. n=6; scale bar, 100μm. For panels **A**–**D**, data are presented in box-and-whiskers plots

showing minimal to maximal values and all data points; for panels **E** and **F**, data are presented in violin plots showing all data points; for panel **K**, data are presented as mean and SEM; for panel **G**, data are presented by Kaplan-Meier survival plot; for panel I, data are presented as mean and SEM; Mann-Whitney test for panels **A**, **B**, **E**, **F** and **K**; Kruskal-Wallis test for panels **C**, **D** and **I**; ns, not significant, *p< 0.05, **p < 0.01, ***p<0.001.

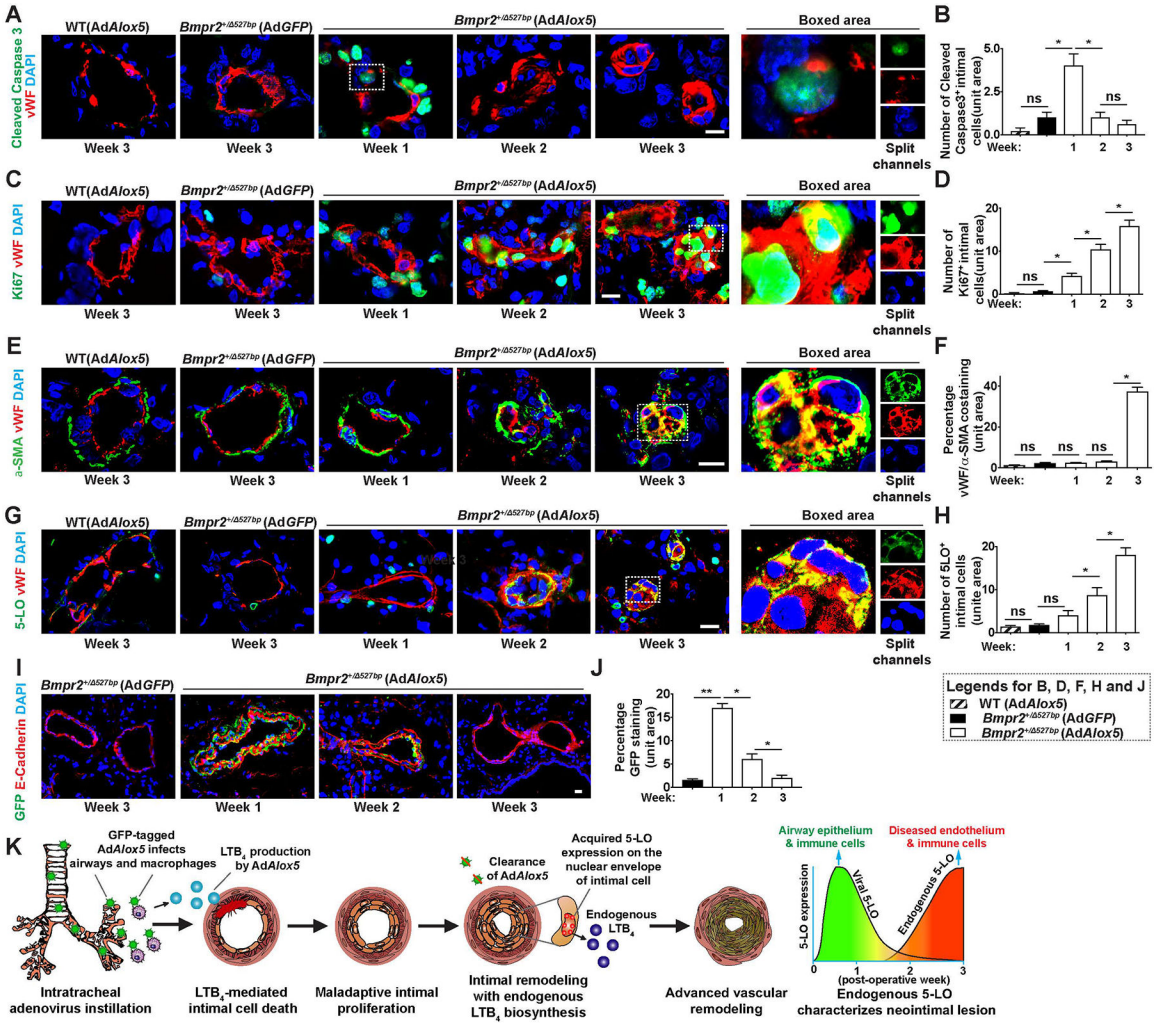

Figure 2. Transient Ad*Alox5* infection generates a remodeled neointima which expresses endogenous non-viral 5-LO.

Representative immunofluorescent confocal images and quantification of lung sections collected weekly following viral instillation. (**A** and **B**) Distal pulmonary arterioles (PAs) were stained with early apoptosis marker, cleaved caspase 3 (green) and endothelial marker, von Willebrand factor (vWF, red). Boxed area with split channels highlights intimal cell injury 1 week after viral injection. n=6; scale bar, 50μm. (**C** and **D**) Representative confocal staining and quantification of Ki67 (green) expressing proliferative vWF^{+} (red) cells. Boxed area with split channels indicates neointimal proliferation at postoperative week 3. n=6; scale bar, 50μm. (**E** and **F**) Representative images and quantification of α-SMA (green) and vWF (red) staining. Colocalization of α-SMA and vWF in the obliterative lesion is highlighted. n=6; scale bar, 50μm. (**G** and **H**) Representative images and quantification of 5-LO (green) and vWF (red) costaining. Boxed area with split channels demonstrates endogenous 5-LO expression in the transformed neointima. Note the nuclear envelope localization of 5-LO. n=6; scale bar, 50μm. (**I** and **J**) Representative images and quantification of GFP-tagged virus (GFP, green) and epithelium marker, E-Cadherin (red) staining. Note GFP-tagged adenoviral particles are located in the airway epithelium 1 week

after infection and gradually receded. n=6; scale bar, 50μm. (**K**) Proposed model: GFP-labeled Ad*Alox5* infects airway epithelium and alveolar macrophages after intratracheal instillation and secretes LTB_4. Exogenous LTB_4 diffuses to PAs and causes intimal cell apoptosis. Maladaptive intimal cell proliferation forms the neointima, which expresses endogenous 5-LO with *de novo* synthesis of LTB_4 independent of viral activities. Extensive vascular remodeling in advanced disease features an obliterative and proliferative intima with signature of endothelium to mesenchymal transition (EndMT). As adenoviral 5-LO disappears from the lung, it is replaced by endogenous 5-LO which is sustained. DAPI (blue) identifies nuclei. Data are presented as means and SEM; Kruskal-Wallis test; ns, not significant, *$p< 0.05$, **$p < 0.01$.

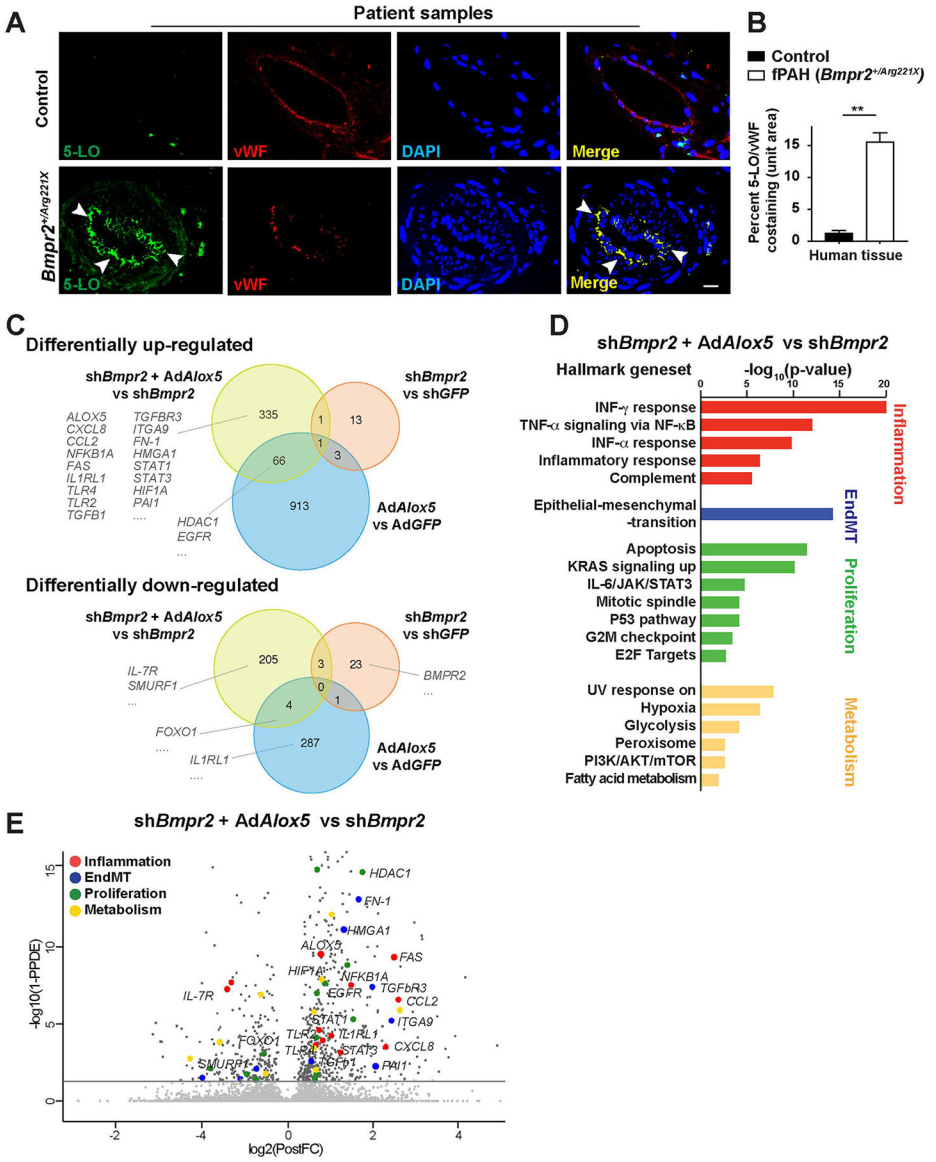

Figure 3. The *Bmpr2* mutant hPAH neointima is characterized by 5-LO expressing cells with a unique RNA transcriptome.

(**A** and **B**) Representative confocal images and quantification of pulmonary arteries in lung tissue sections collected from donor controls or hPAH patients and stained for 5-LO (green) and vWF (red). DAPI (blue) identifies nuclei. White arrow heads point to the 5-LO^{+}/vWF^{+} cells in the center of the vascular lesion. n=11 for control subjects; n=19 for the hPAH samples; scale bar, 50μm. Data are expressed as means and SEM; Mann-Whitney test; **p < 0.01. (**C**–**E**) RNAseq analysis of human control pulmonary artery endothelial cells (PAECs) cultured with lentivirus expressing *Bmpr2*-targeted short hairpin RNA (sh*Bmpr2*) and treated with or without Ad*Alox5* for 7 days. Cells treated with Ad*Alox5* alone were assessed to model the effects of increased 5-LO-mediated inflammation. PAECs in culture of GFP expressing adenovirus (Ad*GFP*) or GFP-targeted lentiviral shRNA (sh*GFP*) served as vector control groups. Genes with average fold-differences greater than or equal to 50% were curated for comparisons. (**C**) Venn diagram based on dataset comparisons between

sh*Bmpr2+*Ad*Alox5* versus sh*Bmpr2*, sh*Bmpr2* versus sh*GFP* and Ad*Alox5* versus Ad*GFP* treatment groups. Numbers of differentially expressed genes (DEGs) in each treatment group are presented. Threshold of false discovery rate <0.05. (**D**) Hallmark geneset enrichment analysis of sh*Bmpr2+*Ad*Alox5* versus sh*Bmpr2* treatment groups showing the most significantly upregulated pathways. (**E**) Volcano plot with representative DEGs in the sh*Bmpr2+*Ad*Alox5* versus sh*Bmpr2* comparisons. DEGs implicated in inflammatory responses, cell proliferation, EndMT and cell metabolism are highlighted.

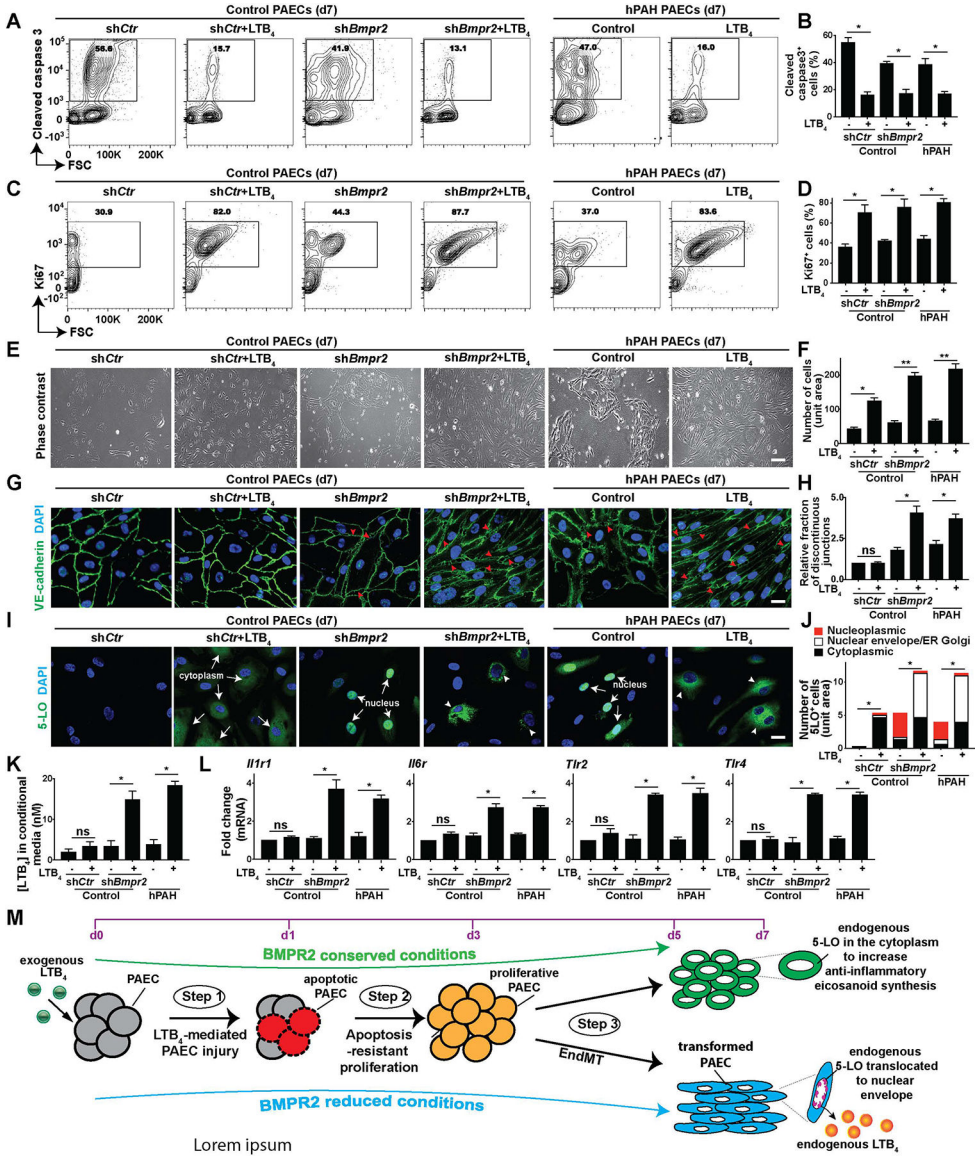

Figure 4. BMPR2 deficiency coupled with increased 5-LO-mediated immunity induces a proliferative and inflammatory endothelial phenotype.

To mimic BMPR2 signaling loss *in vitro*, PAECs from control donor were infected with lentiviral sh*Bmpr2* or control lentivirus (sh*Ctr*) and were compared with cells collected from hPAH patient bearing *Bmpr2* mutations. PAECs were subsequently cultured in 400nM LTB_4 or vehicle in the serum free medium for 7 days to assess the effects of increased 5-LO-mediated inflammation. (**A** and **B**) Representative flow cytometry contour plots and quantification of cleaved caspase 3. n=6. (**C** and **D**) Representative flow cytometry contour plots and quantification of Ki67. n=6. (**E** and **F**) Representative PAEC phase-contrast light microscopy images and quantification. n=6; scale bar, 100μm. (**G** and **H**) Representative confocal images and quantification of cells stained with tight junction marker, VE-cadherin (green). DAPI (blue) identifies nuclei. Red arrow heads point to the discontinuous cellular junctions in **G**. n=6. Scale bar, 100μm. (**I** and **J**) Representative confocal staining and quantification of 5-LO (green). DAPI (blue) identifies nuclei. White arrows point to

endogenous 5-LO expression in the cytoplasm or in the nucleus in **I**; white arrow heads indicate the nuclear envelope and ER and Golgi membrane localized 5-LO in **I**. n=6. Scale bar, 100μm. (**K**) Measurements of leukotriene B4 (LTB_4) in PAEC culture medium. n=6. (**L**) Quantification of *Illrl* (interleukin 1 receptor 1), *Il6r* (IL6 receptor), *Tlr2* (Toll-like receptor 2) and *Tlr4*. (**M**) Model of PAEC transformation: enhanced 5-LO/LTB_4 inflammatory responses cause a step-wise transformation of PAECs with compromised BMPR2 signaling. 1) LTB_4 induces PAEC apoptosis within 24hrs of culture. 2) The surviving, apoptosis-resistant cells become hyperproliferative on day 3, and then 3) transform into a mesenchymal-cell like phenotype on day 5. These cells acquire nuclear envelope-localized 5-LO to produce endogenous LTB_4 and express molecular signature of IL-1, IL-6 and TLR inflammatory pathways. BMPR2-conserved PAECs with LTB_4 culture do not under undergo the inflammatory transformation. All data are presented as means and SEM; Kruskal-Wallis test; ns, not significant, *$p < 0.05$, **$p < 0.01$.

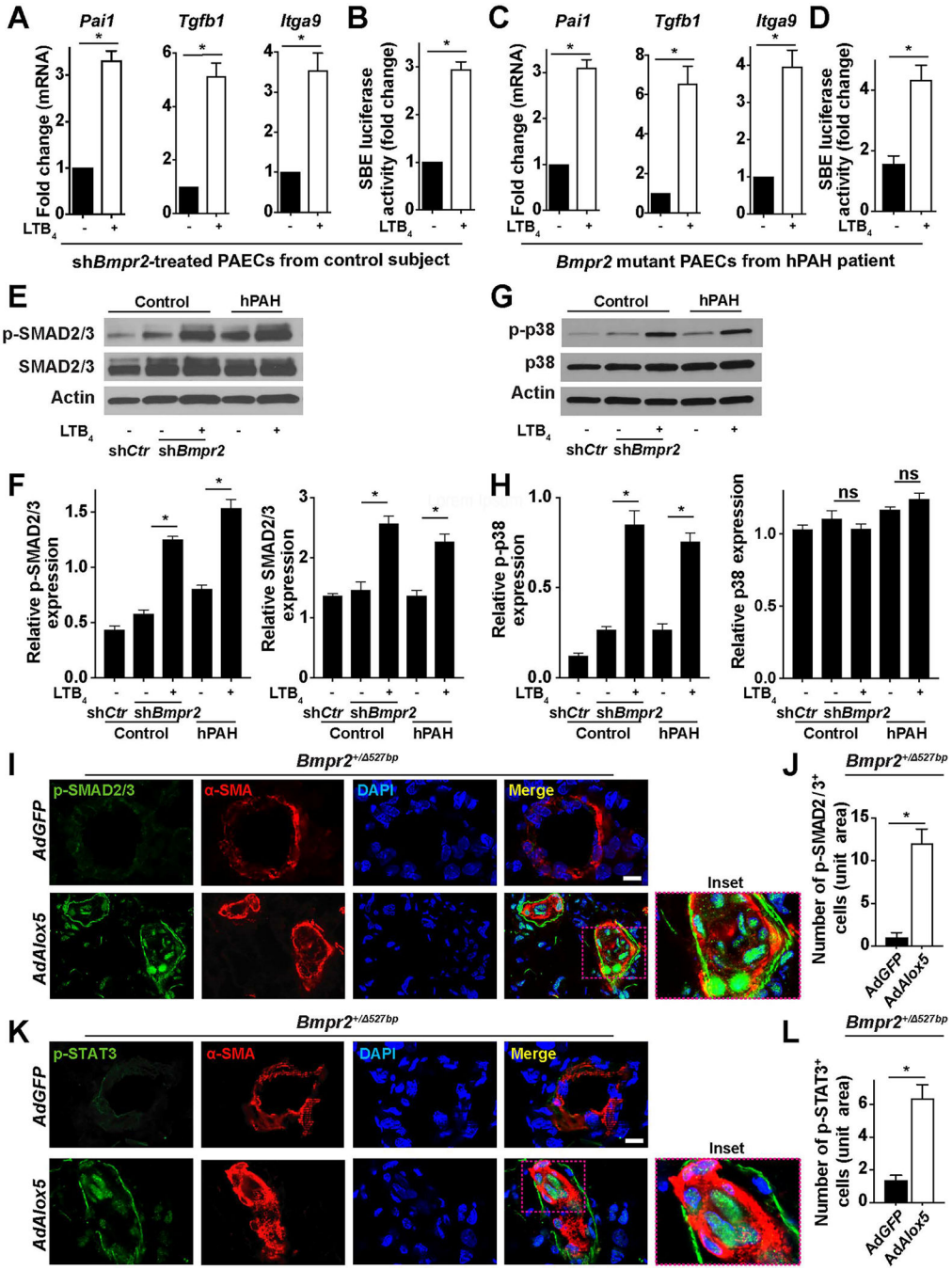

Figure 5. Attenuated BMPR2 signaling promotes TGF-β activation in PAECs following exposure of LTB_4.

(**A**) RNA transcription of *Pail, Tgfβ1* and *Itaga9* in human control PAECs assessed by qPCR on day 7. n=6. (**B**) SBE (SMAD binding element)-mediated reporter assays. n=6. (**C**) RNA transcription of *Pail, Tgfβ1* and *Itaga9* in hPAH-PAECs assessed by qPCR on day 7. n=6. (**D**) SBE-mediated reporter assays. n=6. (**E** and **F**) Representative western blots and densitometry quantification of phosphorylated-(p-) SMAD2/3 and SMAD2/3. n=3. (**G** and **H**) Representative western blots and densitometry quantification of p-p38 and p38. n=3. (**I**–

L) Representative immunofluorescent images and quantification of lung sections stained with p-SMAD2/3 (green, **I**) or p-STAT3 (green, **K**). α-SMA (red) identifies pulmonary vessels. Insets identify the transformed neointima. DAPI (blue) counter-stains nuclei. n=6 for each group; scale bar, 50μm. All data are presented as mean and SEM; for panels **A**–**D**, **J** and **L**, Mann-Whitney test; for panels **F** and **H**, Kruskal-Wallis test; ns, not significant, *p< 0.05.

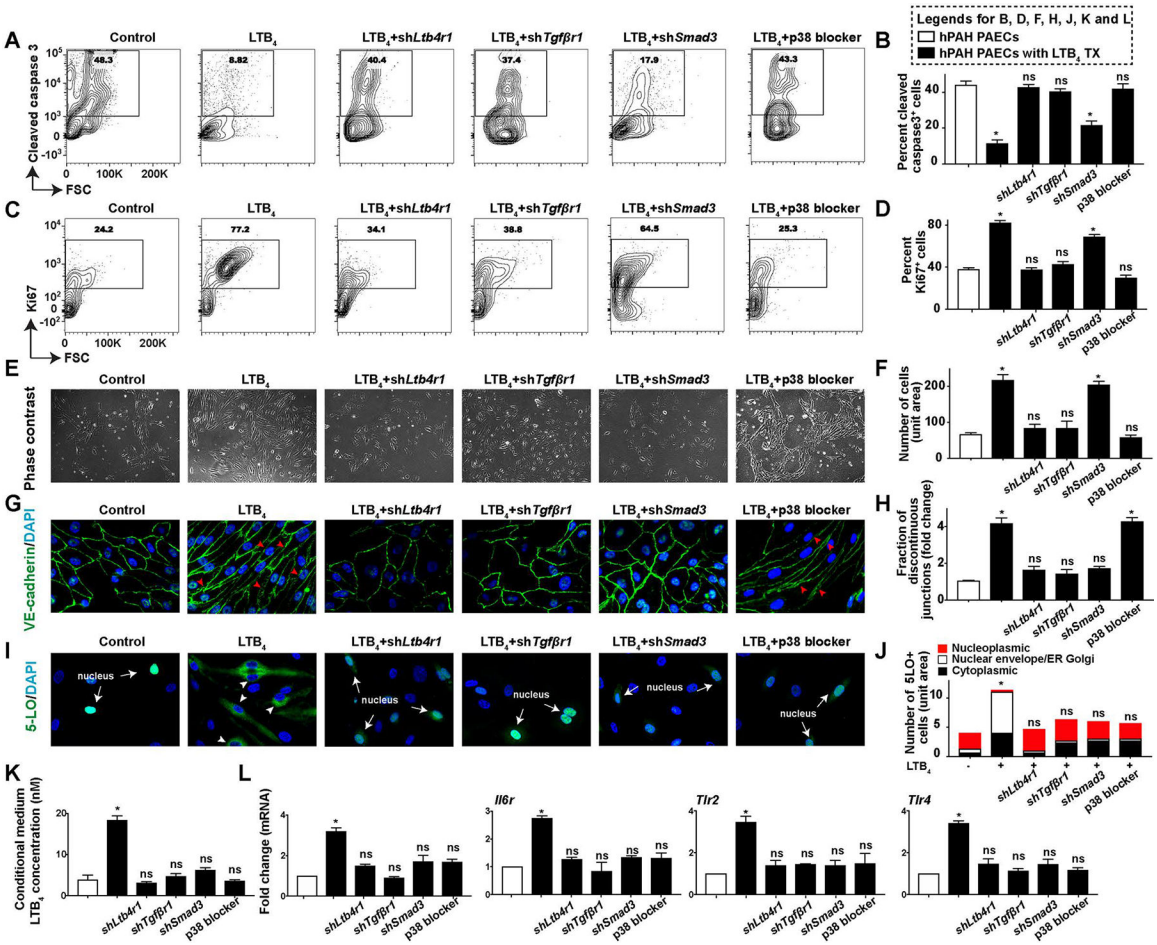

Figure 6. The transformation of BMPR2-defective PAECs requires LTB_4-induced canonical and noncanonical TGF-β signaling.

PAECs from a hPAH patient were either infected with lentivirus of sh*Ltb4r1* (shRNA targeting LTB_4 receptor 1, LTB_4RI), sh*Tgfβr1* (shRNA silencing TGF-β receptor 1, TGFβR1), sh*Smad3*, or were treated with a p38 blocker (SB203580, 1uM). All measurements were carried out 7 days post-treatment. (**A** and **B**) Representative flow cytometry contour plots and quantification of hPAH-PAECs stained for cleaved Caspase 3. n=6. (**C** and **D**) Representative flow cytometry contour plots and quantification of cells stained for Ki67. n=6. (**E** and **F**) Representative phase-contrast light microscopy images and quantification. n=6. Scale bar, 100μm. (**G** and **H**) Representative confocal images and quantification of cells stained with VE-cadherin (green). DAPI (blue) identifies nuclei. Red arrow heads point to the discontinuous cellular junctions in **G**. n=6. Scale bar, 100μm. (**I** and **J**) Representative confocal staining and quantification of 5-LO (green). DAPI (blue) identifies nuclei. White arrows point to endogenous 5-LO expression in the nucleus in **I**; white arrow heads indicate the nuclear envelope and ER and Golgi membrane localized 5-LO in **I**. n=6. Scale bar, 100μm. (**K**) Measurements of LTB_4 in the culture medium. n=6. (**L**) Transcripts of *Illr1, Il6r, Tlr2* and *Tlr4*. n=6. All data are presented as mean and SEM; Kruskal-Wallis test between inhibitor treatment groups versus vehicle control groups (white bar); ns, not significant, *p<0.05.

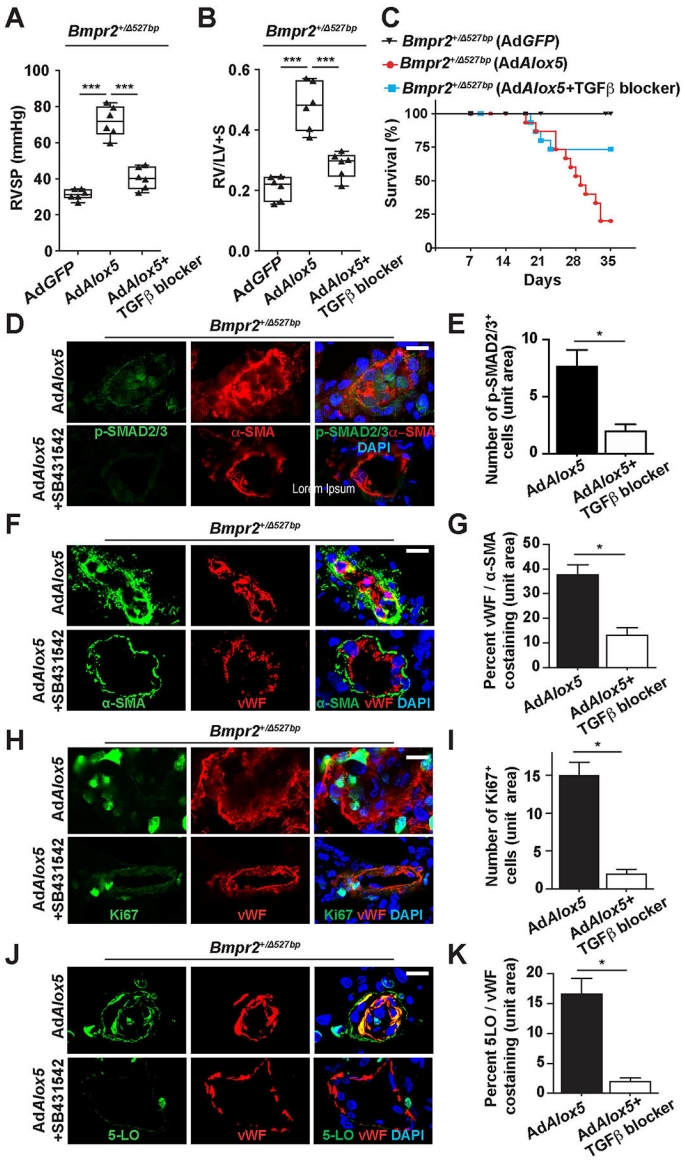

Figure 7. Blocking TGF-β signaling attenuates PAH in the *Bmpr2* m utant rats.

(**A**–**C**) Assessments of RVSP (**A**), RV/LV+S ratio (**B**) and percentage of survival (**C**) of *Bmpr2*$^{+/\Delta 527bp}$ rats treated with a TGFβR1 inhibitor (SB431542) for 2 weeks beginning 3 weeks following Ad*Alox5* delivery. Hemodynamics measurements were performed at post-operative week 5. (**D**–**K**) Representative immunofluorescent images and quantification of distal PAs stained for p-SMAD2/3 (green, **D**), μ-SMA (green, **F**), Ki67 (green, **H**) and 5-LO (green, **J**). vWF identifies vascular endothelium. DAPI (blue) counter-stains nuclei. n=6; scale bar, 50μm. For panels **A** and **B**, data are presented in box-and-whiskers plots showing minimal to maximal values and all data points, Kruskal-Wallis test; for panel **C**, data are presented by Kaplan-Meier survival plot; for panels **E**, **G**, **I** and **K**, data are presented as mean and SEM, Mann-Whitney test; ns, not significant, *p<0.05, ***p<0.001.

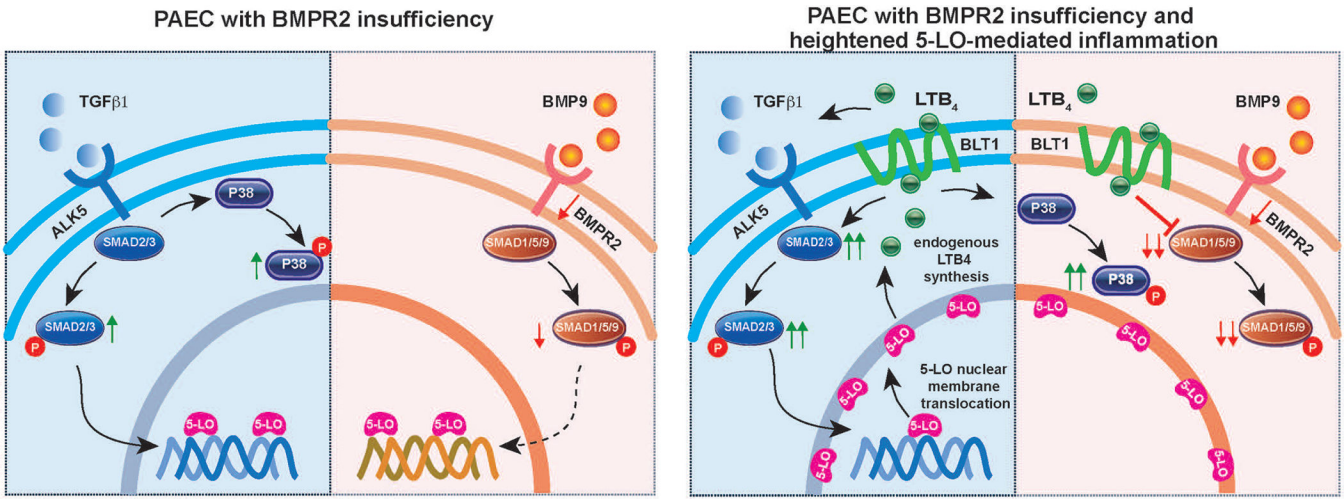

Figure 8. Pathogenic endothelial signaling in 'two-hit' model of disease.

TGFβ1 and BMP9-mediated signaling are compared with and without 5-LO-mediated inflammation. (BMP9 is the principal high-affinity ligand for canonical BMPR2 signaling.[4]) BMPR2 insufficiency creates a proclivity for enhanced canonical and noncanonical TGFβ signaling, and increased 5-LO nucleoplasmic expression. 5-LO-mediated inflammation activates SMAD2/3-dependent canonical and p38-dependent noncanonical TGF-β pathways, inhibits SMAD1/5/9-mediated BMPR2 signaling, augments 5-LO nuclear envelope translocation for endogenous LTB_4 synthesis and promotes PAEC pathological transformation.